Sulfur dimers adsorbed on Au(111) as building blocks for sulfur octomers formation: A density functional study

Carlos E. Hernandez-Tamargo, Ana Lilian Montero-Alejo, Daniel Codorniu Pujals, Hans Mikosch, and Mayra P. Hernández

Citation: The Journal of Chemical Physics **141**, 044713 (2014); doi: 10.1063/1.4890997
View online: http://dx.doi.org/10.1063/1.4890997
View Table of Contents: http://scitation.aip.org/content/aip/journal/jcp/141/4?ver=pdfcov
Published by the AIP Publishing

Articles you may be interested in

Barrier height formation in organic blends/metal interfaces: Case of tetrathiafulvalene-tetracyanoquinodimethane/Au(111)
J. Chem. Phys. **139**, 214706 (2013); 10.1063/1.4836635

Spin polarization study of graphene on the Ni(111) surface by density functional theory calculations with a semiempirical long-range dispersion correction
J. Appl. Phys. **114**, 143713 (2013); 10.1063/1.4824186

C58 on Au(111): A scanning tunneling microscopy study
J. Chem. Phys. **138**, 104703 (2013); 10.1063/1.4793761

Structure and thermal fluctuation of one-dimensional AgO chains on Ag(110) surfaces studied with density functional theory and Monte Carlo simulations
J. Chem. Phys. **129**, 154709 (2008); 10.1063/1.2993251

A density functional theory study of the adsorption of sulfur, mercapto, and methylthiolate on Au(111)
J. Chem. Phys. **116**, 784 (2002); 10.1063/1.1424292

AIP Journal of Applied Physics

Journal of Applied Physics is pleased to announce André Anders as its new Editor-in-Chief

This article is copyrighted as indicated in the article. Reuse of AIP content is subject to the terms at: http://scitation.aip.org/termsconditions. Downloaded to IP: 128.131.138.244 On: Wed, 30 Jul 2014 14:47:22

Sulfur dimers adsorbed on Au(111) as building blocks for sulfur octomers formation: A density functional study

Carlos E. Hernandez-Tamargo,[1] Ana Lilian Montero-Alejo,[1] Daniel Codorniu Pujals,[2] Hans Mikosch,[3] and Mayra P. Hernández[4,a)]

[1]*Laboratory of Computational and Theoretical Chemistry (LQCT), Faculty of Chemistry, Havana University, Havana 10400, Cuba*
[2]*Higher Institute of Technologies and Applied Sciences (InSTEC), Havana 10400, Cuba*
[3]*Institute of Chemical Technologies and Analytics, Vienna University of Technology, Getreidemarkt 9/E164-EC, 1060 Vienna, Austria*
[4]*Instituto de Ciencias y Tecnologías de Materiales (IMRE), Havana 10400, Cuba*

(Received 6 April 2014; accepted 11 July 2014; published online 30 July 2014)

Experimental scanning tunneling microscopy (STM) studies have shown for more than two decades rectangular formations when sulfur atoms are deposited on Au(111) surfaces. The precursors have ranged from simple molecules or ions, such as SO_2 gas or sulfide anions, to more complex organosulfur compounds. We investigated, within the framework of the Density Functional Theory, the structure of these rectangular patterns assuming them entirely composed of sulfur atoms as the experimental evidence suggests. The sulfur coverage at which the simulations were carried out (0.67 ML or higher) provoked that the sulfur-sulfur association had to be taken into account for achieving a good agreement between the sets of simulated and experimental STM images. A combination of four sulfur dimers per rectangular formation properly explained the trends obtained by the experimental STM analysis which were related with the rectangles' size and shape fluctuations together with sulfur-sulfur distances within these rectangles. Finally, a projected density of states analysis showed that the dimers were capable of altering the Au(5d) electronic states at the same level as atomic sulfur adsorbed at low coverage. Besides, sulfur dimers states were perfectly distinguished, whose presence near and above the Fermi level can explain both: sulfur-sulfur bond elongation and dimers stability when they stayed adsorbed on the surface at high coverage. © *2014 AIP Publishing LLC*. [http://dx.doi.org/10.1063/1.4890997]

I. INTRODUCTION

Since the beginning of the 1990s, peculiar scanning tunneling microscopy (STM) images related to the deposition of sulfur atoms on Au(111) surfaces have been the focus of attention of numerous papers about surface science.[1–12] Those images show rectangular formations and the atomic resolution allows to distinguish eight atomic centers per rectangular structure.[3,8–10] As precursors for sulfur deposition, the list ranges from sulfide anions in aqueous solutions[2–4,7] to gaseous molecules such as sulfur dioxide[5,6] to organosulfur compounds[8–12] which decompose on the Au(111) surface leaving the sulfur atoms free.

The interpretations of these formations have been split. On one hand, the presence of rectangles in the STM images has been explained by Biener *et al.*[5,6] through a stoichiometric 2D Au-S phase created on top of the Au(111) surfaces. These authors use a gas phase of sulfur dioxide as sulfur carrier, finding the lifting of the Au(111) surface herringbone reconstruction at the earlier stages of sulfur deposition (sulfur coverage 0.1 ML). The unreconstructed Au(111) surface remains stable up to approximately 0.3 ML when a $\sqrt{3} \times \sqrt{3}$ superlattice is detected by low energy electron diffraction (LEED). Beyond 0.3 ML, the STM images show monoatomic etch pits and islands formations whose densities increase with sulfur coverage. The etch pits are interpreted by the authors as evidence of Au(111) corrosion induced by the deposited sulfur atoms, meanwhile the islands are related with the formation of the superficial Au-S phase. These Au-S islands form aggregates with sponge-like appearance upon sulfur coverage of 0.6 ML, which passivates the Au(111) surface against further corrosion. When this surface is annealed at 450 K, the STM images show the aforementioned rectangular formations with long range ordering detected by LEED experiments. The proposed Au-S phase exhibits a 1:1 stoichiometry, obtained by correlating auger electron spectroscopy (AES) information, which gives sulfur coverage of about 0.5 ML, with STM images analysis, which shows island vacancies leading to an estimation of gold atoms within the Au-S phase of approximately 0.5 ML.

On the other hand, it has been considered that rectangles are formed by entities of eight sulfur atoms (a sulfur octomer).[2–4,7–12] Lustemberg *et al.*[7] perform one of the most extended studies that sustains this approach supported by STM and X-ray photoemission spectroscopy (XPS) as well as electrochemistry experiments and surface enhanced Raman spectroscopy (SERS). This work and those previously reported by Vericat *et al.*[3,4] use an aqueous solution of sodium sulfide and sodium hydroxide at room temperature, verifying the oxidation and deposition of sulfide anions on the Au(111) surface. The experimental evidences withdraw the possibility

a)Author to whom correspondence should be addressed. Electronic mail: mayrap@imre.oc.uh.cu

 © 2014 AIP Publishing LLC

This article is copyrighted as indicated in the article. Reuse of AIP content is subject to the terms at: http://scitation.aip.org/termsconditions. Downloaded to IP: 128.131.138.244 On: Wed, 30 Jul 2014 14:47:22

of superficial Au-S phase formation since they are unable for detecting oxidized gold. Instead, the results are consistent with an arrangement of monomeric and polymeric species of sulfur atoms directly bonded to the surface gold atoms.

The rectangular patterns have also been observed in STM images when solutions of organosulfur compounds have been put in contact with Au(111) surfaces. The reports include hexamethyldisilathiane,[8] and different substituted arene sulfonyl phthalimides[11] as well as dithiobisphthalimide,[9] triphenylmethane sulfenyl chloride[10] and thiobis-(hexamethyldisilazane).[12] In these cases, XPS experiments are only able to detect the $2p_{3/2}$ sulfur signals and there are no peaks that could indicate the presence of other entities on the surface such as silicon atoms and aromatic or phthalimide moieties. These facts are explained by the authors considering the cleavage of bonds in the molecules which frees the sulfur atoms on the Au(111) surfaces. Consequently, they also propose arrangements of eight sulfur atoms directly absorbed on Au(111) in order to explain the rectangular structure.

Nevertheless, theoretical studies of rectangles formation have been less numerous than the experimental ones; two relevant works have been carried out. The first one,[13] which is based on the experimental results of Biener *et al.*,[5] uses the density functional theory (DFT) at the PW91 level[14] to propose a 2D Au-S phase with 1:1 stoichiometry. The periodicity of this phase is described by an incommensurate supercell whose dimensions are consistent with the experimental measures.[5] The 2D supercell contains four gold and four sulfur atoms with different coordination environments. The analysis of the bond structure using localized Wannier functions[15] suggests the absence of strong directional bonds between the 2D phase and the Au(111) surface. The authors attribute the stability of the 2D phase to the reduction in surface energy and to the charge transfer from Au(111) to the Au-S phase. However, their simulated STM images do not clearly coincide with those reported in other experimental works where the rectangles and the atomic centers at high resolution are easily defined.[3,8–12]

The second work, by Lustemberg *et al.*,[7] is a DFT calculation at the PW91 level[14] which complements the experimental study performed by these authors. The theoretical simulation uses a three-layer slab with $3 \times 2\sqrt{3}$ periodicity in order to represent the Au(111) surface and eight sulfur atoms are placed on its high symmetry positions. It is only presented the most stable model after relaxation which consists in a mixture of sulfur dimers and monomers and whose simulated STM image shows a clear rectangular pattern. This is consistent with the experimental results given in this same work. This report is mainly focused on demonstrating that sulfur atoms are not able to create strong corrosion on the Au(111) surfaces at high coverage. Therefore it lacks of a systematic treatment that could explain the variations in octomers shape and size that appear in real STM images.[3,7,9,10]

The present work has been focused on providing feasible atomistic models for representing rectangular structures adsorbed on Au(111) surfaces by means of a DFT study. The proposed models were centered exclusively on sulfur-gold interaction following the XPS results which highlight the sulfur element as the main species adsorbed on the surface.[4,7] Although other compounds (sodium hydroxide[2,3,7] and side products of organosulfur molecules decomposition[8–12]) are present in the solution during the sulfur deposition, there is no experimental evidence that could clarify if other species are adsorbed on Au(111) together with the sulfur atoms. Therefore, as a first step for studying these systems, we remained close to the standard proposition which consists solely on sulfur atoms adsorbed on Au(111).

At first, we demonstrated that the view of beginning with single sulfur atoms adsorbed on high symmetry positions of the Au(111) surface was not adequate to achieve rectangular patterns. Then, we appealed to four sulfur dimers as building blocks to form each octomer on the Au(111) surface. Several structures were obtained with different arrangements of dimers and the corresponding STM images were simulated. Having the structures that could properly explain these formations, a close up to their electronic structure was achieved through projected density of states (PDOS) analysis.

Therefore, we have given a complete explanation for the sulfur octomers formation. Our models based on four sulfur dimers were supported by the experimental evidence: XPS,[4,7,9,16] SERS,[7] and thermal desorption mass spectroscopy (TDS)[16] experiments highlight the presence of sulfur polyatomic aggregates on the Au(111) surfaces within the conditions for octomers formation.

II. DFT CALCULATIONS

The calculations were performed in the framework of the DFT code VASP.[17–20] The exchange-correlation functional was described within the generalized gradient correction (GGA) using the proposition of Perdew, Burke and Ernzerhof (PBE).[21] The van der Waals (vdW) interactions were included through the semiempirical method of Grimme;[22] in this case, the gold coefficients calculated by Toyoda *et al.*[23] ($C_6 = 47.81\,\mathrm{Jnm^6\,mol^{-1}}, R_0 = 1.497\,\text{Å}$) were used. The description of the nodal features of the valence electrons eigenfunctions and their interaction with the inner region of the atoms were carried out with the projected augmented wave method (PAW);[24,25] meanwhile plane wave basis sets were used to expand these eigenfunctions. The first Brillouin zone (BZ) was mapped using the Monkhorst and Pack method.[26] The convergence of the band structure calculation was improved by means of Methfessel and Paxton smearing method[27] with $\sigma = 0.2$ eV.

The calculated equilibrium separation between neighboring gold atoms in the bulk was 2.96 Å at the PBE level, close to the experimental value 2.88 Å. The Au(111) surface was described using the slab model with four layers of gold atoms. The number of layers within the slab was established attending a convergence process prior to the development of the present work (see the supplementary material[42] for details). The thickness was varied from one to nine layers using a $3 \times 2\sqrt{3}$ periodicity for the slabs. The sulfur-sulfur and sulfur-gold distances as well as the adsorption energy served as variables for measuring the convergence. During this process, a single sulfur atom or a single sulfur dimer were deposited on each surface and allowed to relax. In consequence, the fluctuations on the distances and the adsorption energies

This article is copyrighted as indicated in the article. Reuse of AIP content is subject to the terms at: http://scitation.aip.org/termsconditions. Downloaded to IP: 128.131.138.244 On: Wed, 30 Jul 2014 14:47:22

remained below 0.01 Å and 0.05 eV, respectively, from three layers onwards. Therefore, a four-layer slab gave the necessary balance between accuracy and computing time consumption taking into account that some tested models could reach thirty gold atoms per layer. Further tests were performed using a six-layer slab with the rectangular structures presented here, which have a higher coverage than those models used in the initial convergence process. This final check did not show any significant variation that could have invalidated the four-layer election. A vacuum layer with 20 Å of thickness was placed immediately above the slab ensuring negligible interactions between periodic images in the normal direction to the surface. The van der Waals corrections were only considered for those interactions between pair of atoms separated by a distance up to 15 Å. The sulfur atoms were placed on one side of the slab; owing to this asymmetry, a dipole moment correction was introduced to improve the convergence. In all calculations, the positions of the gold atoms in the two bottom layers were kept fixed in order to simulate the bulk region. The structures were relaxed with a $6 \times 6 \times 1$ k-point sampling and cutoff energy of 400 eV. The convergence thresholds for the electronic self-consistent field (SCF) iterations and ionic forces were held on 10^{-5} eV and 0.03 eV/Å, respectively. All previous calculations were performed without spin polarization due to the invariability of the final results if this correction is taken into account.

The STM images were obtained from the p4vasp software[28] within the Tersoff-Hamann approach[29] using the partitioned charge density given by VASP (LPARD, NBMOD, and EINT parameters). The images were generated in constant current mode. The states considered in the partitioned charge density were within 100 meV above and below the Fermi level.

The adsorption energy per sulfur atom when they adsorb on a bare Au(111) surface was calculated according to the following equation:

$$E_{ads} = (E_{S_n/Au(111)} - E_{Au(111)} - nE_S)/n, \qquad (1)$$

where $E_{S_n/Au(111)}$ is the energy of n sulfur atoms adsorbed on the Au(111) slab, $E_{Au(111)}$ is the energy of the clean Au(111) slab and E_S is the energy for an isolated sulfur atom in the center of a cell with dimensions $20 \times 21 \times 22$ Å^3. The spin polarization was taken into account for the isolated sulfur atom calculation.

The adsorption energy per additional sulfur atom that adsorbs on a Au(111) surface with pre-adsorbed sulfur atoms was calculated according to the following equation:

$$E_{ads} = (E_{S_{m+n}/Au(111)} - E_{S_n/Au(111)} - mE_S)/m, \qquad (2)$$

where $E_{S_{m+n}/Au(111)}$ and $E_{S_n/Au(111)}$ are the energies of $m + n$ and n sulfur atoms adsorbed on the Au(111) slab, respectively, being m the number of additional and n the number of pre-adsorbed sulfur atoms.

III. DFT RESULTS

Figure 1 shows the models based on two schemes that have been reported in previous experimental works to explain how the sulfur atoms are ordered to form the octomers.[3,10] Both schemes place eight individual sulfur atoms on high symmetry positions of the Au(111) surface, arranging them with rectangular shape. One of the scheme is proposed by Vericat *et al.*,[3] which considers that three sulfur atoms are adsorbed on fcc, three on hcp and two on top positions making use of a supercell with periodicity $3 \times \sqrt{13}$ (O1-A in Figure 1). In addition, we proposed five additional structures, which conserved the rectangle size reported by Vericat but with different combinations of the high symmetry positions. Two of them used the same supercell (O1-B and O1-C in Figure 1) and the other three were reproduced with a periodicity of $3 \times 2\sqrt{3}$ (O1-D, O1-E, and O1-F in Figure 1). The O1-E and O1-F models are very similar to that reported by Lustemberg *et al.*[7] for their DFT simulation. The other scheme is that used by Houmam *et al.*,[10] where the sulfur atoms are placed on top and bridge positions within a $3 \times \sqrt{7}$ supercell (O1-G and O1-H in Figure 1). Two extra formations were proposed following this idea: O1-I and O1-J, where different high symmetry position arrangements were tested.

Figure 2 shows the simulated STM images after the structural optimization of the models illustrated in Figure 1. As

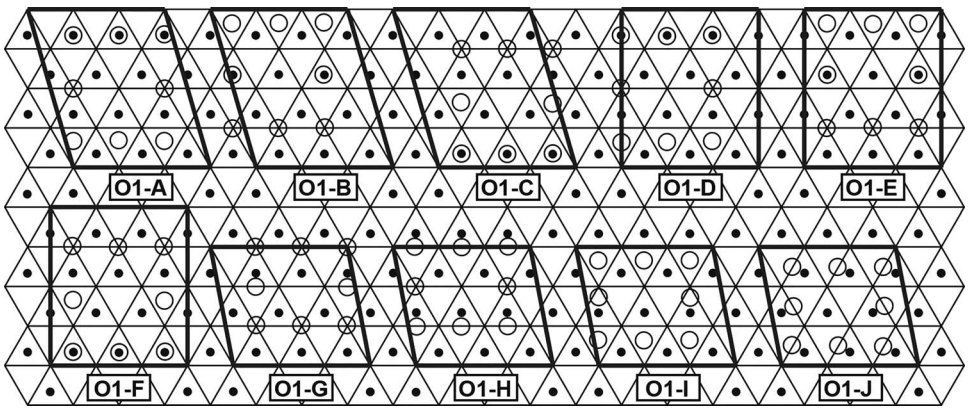

FIG. 1. Schemes that illustrate the octomers formation through the arrangement of eight individual sulfur atoms at high symmetry positions on the Au(111) surface. The Au(111) surface is represented by the triangles in solid line: the gold atoms are represented by the corners of the triangles and the black circles represent the hcp positions. The open circles correspond to the sulfur atoms. Beneath each model is the label that identifies it. Three periodicities are used: $3 \times \sqrt{13}$ (O1-A, O1-B, and O1-C, surface coverage of 0.67 ML), $3 \times 2\sqrt{3}$ (O1-D, O1-E, and O1-F, surface coverage of 0.67 ML) and $3 \times \sqrt{7}$ (O1-G, O1-H, O1-I, and O1-J, surface coverage of 0.89 ML).

This article is copyrighted as indicated in the article. Reuse of AIP content is subject to the terms at: http://scitation.aip.org/termsconditions. Downloaded to IP: 128.131.138.244 On: Wed, 30 Jul 2014 14:47:22

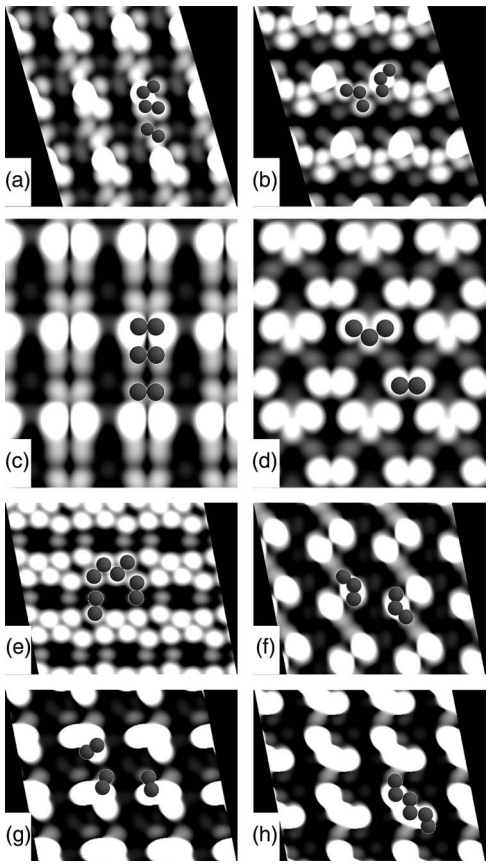

FIG. 2. Simulated STM images from the full relaxed structures in Figure 1. (a) O1-A, (b) O1-B and O1-C, (c) O1-D, (d) O1-E and O1-F, (e) O1-G, (f) O1-H, (g) O1-I, and (h) O1-J. The images are threefold replicated along the axes that are parallel to the surface plane (in the present case *x* and *y* axes). In the images the sulfur atoms of a single supercell are included in dark gray color which form aggregates such as dimers and trimers.

it can be seen, there were formation of polyatomic sulfur species, with sulfur-sulfur distances ranging between 1.9 and 2.0 Å for dimers and between 2.0 and 2.1 Å for trimers. The sulfur dimers and trimers formation was produced by the effect of the high coverage at which the simulations were carried out.[16,30] However, the desired rectangular patterns were not observed in the simulated STM images of Figure 2, being the O1-G model[10] (see Figure 2(e)) the only possible exception in whose image it can be distinguished a rectangle formed by sulfur dimers.

At low and intermediate coverage (lower than 0.33 ML) it is well established by DFT calculations[16,31–33] that sulfur atoms occupy threefold positions on the Au(111) surfaces. In these conditions, they stay on the surface as monoatomic species due to the considerable distance that separates two neighboring sulfur atoms (at least more than twice the sulfur-sulfur bond distance). However, the increment of sulfur coverage produces weakening of the sulfur-gold bonds which changes the stability of the adsorption sites and could lead to sulfur-sulfur bonding, resulting eventually in the adsorption of polyatomic species. This trend has been reported by XPS experiments[4,16] and DFT calculations.[16,30]

Vericat *et al.*,[4] studying the deposition of sulfur atoms on the Au(111) surface from an alkaline solution of sulfide anions, report the transition from monoatomic to polyatomic sulfur phase when the coverage is increased. They relate the XPS S($2p_{3/2}$) doublets at approximately 161.0 and 162.0 eV to monoatomic and polyatomic sulfurs, respectively, directly bonded to the surface gold atoms. The correlation of XPS data with STM images allows them to assign the former doublet to $\sqrt{3} \times \sqrt{3}$ sulfur phase and the latter to sulfur octomers. The authors observe that the relative intensity of $\sqrt{3} \times \sqrt{3}$ signal decreases while that of octomers increases when time exposition to sulfur solution grows. The STM images show equivalent results since the area covered by $\sqrt{3} \times \sqrt{3}$ reduces favoring the growth of the sulfur octomers coverage.

In addition, a combined experimental and theoretical work carried out by Rodriguez *et al.*[16] shows similar conclusions about the association among sulfur atoms at high coverage. Their results of XPS and TDS experiments establish sulfur dimers as the main species on the Au(111) surface when sulfur coverage is close to 1 ML. At the same time, their DFT calculations show that dimerization processes occur spontaneously when coverage ranges from 0.5 to 1 ML, having the dimeric phases bigger adsorption energies on Au(111) than adsorbed monoatomic sulfurs. Meanwhile, charge transfer from Au(111) to sulfur atoms decreases for increasing coverage, ranging from $-0.2e$ for 0.25 ML to almost $0.0e$ for 1 ML; this could have a special significance for dimers formation. Abufager *et al.*[33] calculate Bader charge in sulfur-Au(111) systems of low and intermediate coverage (lower than 0.33 ML), resulting in charge transfer of approximately $0.26e$ towards sulfur atoms. These authors suggest that sulfur-sulfur electrostatic repulsions prevent sulfur atoms approaching each other at distances below 3 Å. However if charge transfer decreases as consequence of coverage increments, the electrostatic impediment (if it really has an important role) is eliminated.

Mankefors *et al.*[30] arrive to similar results about sulfur-sulfur association by means of DFT calculations. The authors studied the adsorption of sulfur and selenium atoms on Au(111) surface from 0.25 to 1 ML. At 0.75 ML, they find that sulfur and selenium trimers or dimers (depending on the starting positions before relaxation) are the energetically most favorable species on the Au(111) surface, being the atoms principally adsorbed on-top positions. The threefold positions are not anymore the most stable at high coverage, resulting in the atoms moving out of it during the relaxation towards on-top positions. This behavior is associated by the authors with decrease in sulfur-gold orbital hybridization due to the reduction of available free charge in the extent that the coverage is increased.[30]

Therefore, for a sulfur coverage as high as those used for studying octomer formation, aggregates of two or more sulfur atoms are the most stable entities on the Au(111) surfaces. As it could be seen above, the transition from monomeric to polymeric sulfur during the relaxation process of the models in Figure 1 brought large rearrangements on the surface which avoided the conservation of the initial rectangular patterns.

Skipping this polymerization was our first step towards feasible models that could explain the octomers. The election was to use sulfur dimers instead of individual sulfur atoms in order to form the rectangles. We proposed nine different

This article is copyrighted as indicated in the article. Reuse of AIP content is subject to the terms at: http://scitation.aip.org/termsconditions. Downloaded to IP: 128.131.138.244 On: Wed, 30 Jul 2014 14:47:22

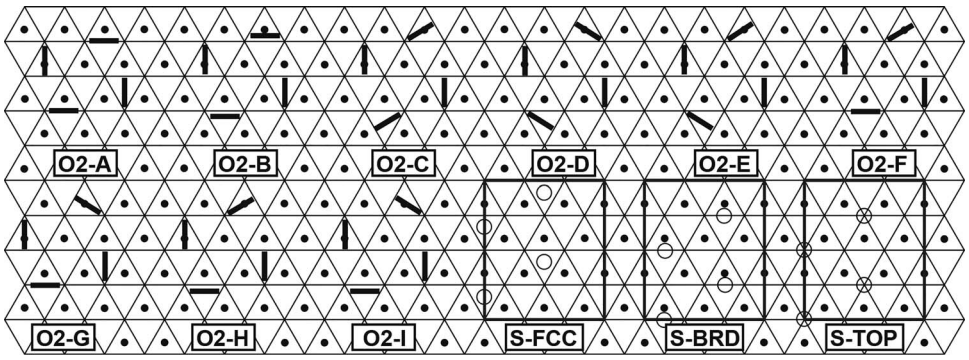

FIG. 3. Schemes that illustrate the arrangements of four sulfur dimers (each dimer is represented by a black bar) to form the octomers and the arrangements of sulfur atoms in $\sqrt{3} \times \sqrt{3}$ superlattices (right bottom). The Au(111) surface is represented by the triangles in solid line, the gold atoms are represented by the corners of the triangles, and the black circles represent the hcp positions. The open circles correspond to the sulfur atoms. Beneath each model is the label that identifies it. The supercell used to replicate the arrangements of sulfur dimers and sulfur atoms on the surface has $3 \times 2\sqrt{3}$ periodicity. The octomer models have a surface coverage of 0.67 ML and the $\sqrt{3} \times \sqrt{3}$ superlattices of 0.33 ML.

orderings of four sulfur dimers forming rectangular pattern on Au(111) slabs with periodicity $3 \times 2\sqrt{3}$. The dimers were placed in three different orientations on Au(111), which were found as the most probable according to our previous calculations: (1) both sulfur atoms are on-top position, (2) both sulfur atoms are on-top position but slightly shifted along the perpendicular direction to the gold-gold bonds, and (3) one sulfur atom is on-top while the other is on bridge position. The new models are shown in Figure 3 where each dimer is represented by a black bar. The O2-A and O2-B models in Figure 3 place their dimers in perpendicular directions trying to reproduce the rectangular patterns without deformations on the STM images. The structures of the deformed octomers that are observed in the experimental STM images[3,7,9,10] were represented by the other seven models (from O2-C to O2-I in Figure 3), which were the result of perturbing the dimers' initial positions in O2-A and O2-B. Besides, three monomeric systems are included in Figure 3 as references to analyze the changes generated by the formation of dimers. Here four sulfur atoms were adsorbed in $\sqrt{3} \times \sqrt{3}$ superlattices and periodically repeated by $3 \times 2\sqrt{3}$ supercells. The $\sqrt{3} \times \sqrt{3}$ superlattices are labeled in Figure 3 as S-FCC, S-BRD, and S-TOP for sulfur atoms adsorbed on fcc, bridge, and top positions, respectively.

Figure 4 displays the simulated STM images obtained after the structural optimization. The *xy* plane coincides with the surface and each image is expanded three times along *x* and *y* axes. Rectangular structures are easily distinguished in the simulated images of the O2-A and O2-B models; the other images can be perfectly associable with the mentioned deformed octomers. As it can be seen in Figure 4, sulfur dimers can be a reliable manner to explain octomers shape and size fluctuations: the dimers change their relative positions but in a way that the rectangular patterns deform but never disappear.

In addition, some atoms (sulfur atoms 1 and 5 in O2-C, sulfur atoms 4 and 5 in O2-H, see Figure 4) are observed less bright than others. These atoms were close to bridge positions on the Au(111) surface. Therefore, the sulfur atoms within the dimers moving from on-top to bridge positions could explain the presence of vacancies in the octomers reported by experimental STM results.[3] In this case the vacancies could be

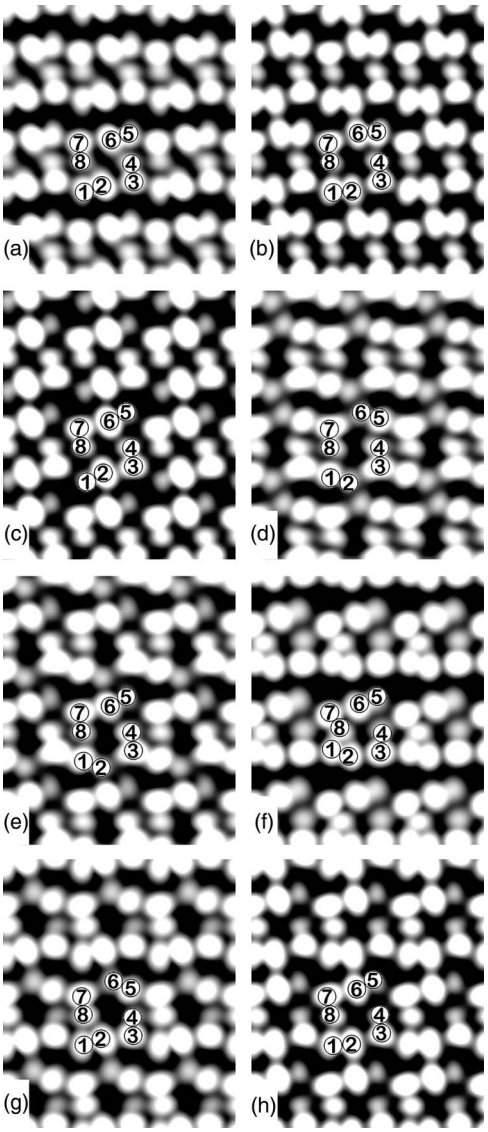

FIG. 4. Simulated STM images from the full relaxed structures in Figure 3. (a) O2-A, (b) O2-B, (c) O2-C, (d) O2-D, (e) O2-E and O2-I, (f) O2-F, (g) O2-G, and (h) O2-H. The images are threefold replicated along the axes that are parallel to the surface plane (in the present case *x* and *y* axes). The sulfur dimers that belong to a single supercell are included in the images as open circles and numerated anti-clockwise.

This article is copyrighted as indicated in the article. Reuse of AIP content is subject to the terms at: http://scitation.aip.org/termsconditions. Downloaded to IP: 128.131.138.244 On: Wed, 30 Jul 2014 14:47:22

TABLE I. Geometric parameters of the complete relaxed structures of the models in Figure 3. $E_{ads.}$, adsorption energy calculated according to Eq. (1) (top value) and Eq. (2) (bottom value). In the case of the energy derived from Eq.(2), S-FCC was taken as the system with pre-adsorbed atoms. Ave. S-S dimers, average sulfur-sulfur distance between two sulfur atoms that form a dimer within the each octomers. Ave. S-S, average sulfur-sulfur distance among all neighboring sulfur atoms. Oct. size, octomer size calculated as the distance among sulfur atoms in each corner of the octomers (see Figure 4 for sulfur atoms numeration). S-Au, distance between a sulfur atom and its closest gold atom on the surface (see Figure 4 for sulfur atoms numeration). Ave. h, average height of the octomers above the Au(111) surface.

	O2-A	O2-B	O2-C	O2-D	O2-E	O2-F	O2-G	O2-H	O2-I	Reference values
$E_{ads.}$ (eV)	−3.60	−3.60	−3.62	−3.62	−3.63	−3.65	−3.62	−3.61	−3.63	−3.92 (S-FCC)
	−3.29	−3.28	−3.32	−3.33	−3.33	−3.39	−3.32	−3.30	−3.34	− 3.56 (S-BRD)
										−2.71 (S-TOP)
Ave. S-S dimers (Å)	2.02	2.04	2.04	2.05	2.04	2.03	2.03	2.04	2.04	1.90[a]
										2.06[b]
Ave. S-S (Å)	2.72	2.74	2.84	2.82	2.84	2.69	2.78	2.79	2.85	2.9 – 3.1[c]
										2.8 – 2.9[d]
Oct. size (Å)										
S1-S3	5.50	5.49	5.34	5.53	5.54	5.37	5.54	5.50	5.37	6.2 ± 0.3, 5.8 ± 0.3[c]
S3-S5	5.30	5.41	5.95	5.28	5.93	6.05	5.28	5.92	5.31	5.9 ± 0.5, 5.1 ± 0.5[d]
S5-S7	5.52	5.50	5.36	5.56	5.37	5.42	5.51	5.36	5.57	5.1 ± 0.1, 5.1 ± 0.1[e]
S7-S1	5.35	5.42	5.94	5.28	5.28	3.99	5.35	5.43	5.94	
S-Au (Å)[f]										
S1-Au	2.40	2.41	**2.46**	2.39	2.39	2.46	2.41	2.40	**2.47**	
S2-Au	2.39	2.39	2.39	**2.48**	**2.47**	2.42	2.42	2.39	2.40	
S3-Au	2.40	2.39	2.41	2.40	2.40	2.38	2.40	2.40	2.40	2.39 (S-FCC)
S4-Au	**2.45**	**2.42**	**2.42**	**2.41**	**2.42**	**2.47**	**2.44**	**2.43**	**2.42**	2.35 (S-BRD)
S5-Au	2.41	2.41	**2.46**	2.39	**2.47**	**2.48**	2.40	**2.46**	2.40	2.23 (S-TOP)
S6-Au	2.39	2.39	2.39	**2.48**	2.39	2.38	**2.48**	2.39	**2.48**	
S7-Au	2.40	2.39	2.41	2.40	2.40	2.46	2.41	2.40	2.40	
S8-Au	**2.46**	**2.42**	**2.43**	**2.42**	**2.43**	2.45	**2.43**	**2.43**	**2.42**	
Ave. h (Å)	2.25	2.23	2.18	2.16	2.17	2.26	2.22	2.20	2.17	1.61 (S-FCC)
										1.78 (S-BRD)
										2.10 (S-TOP)

[a]Current work, isolated sulfur dimer (PBE, 20×21×22 Å^3 supercell).
[b]Current work, isolated S_8 molecule (PBE, square antiprismatic geometry, 20×21×22 Å^3 supercell).
[c]Reference 3.
[d]Reference 9.
[e]Reference 10 (values obtained from STM images analysis).
[f]The values for sulfur atoms close to bridge positions between two gold atoms were set in boldface type. Each given value is the smallest of the two possible sulfur-gold distances.

related to pronounced spot intensities reductions due to adsorption on bridge or even fcc positions.

The results of the nine models after the relaxation are listed in Table I, summarizing geometric parameters, bonding distance, and adsorption energy. The experimental size of the octomers and the sulfur-sulfur distance determined from the STM images[3,9,10] are included for direct comparison with the corresponding calculated values. The values of the monomeric systems shown in Figure 3 (S-FCC, S-BRD, and S-TOP) are also listed, which allows a direct evaluation of the consequences of sulfur-sulfur association.

According to the adsorption energies derived from Eq. (1), the most stable structure was O2-F with −3.65 eV while the least stable were O2-A and O2-B with −3.60 eV (see Table I). This represents a narrow variation which denotes smooth exchange among the nine structures and their simultaneous existence on the surface. However, as the STM and XPS experiments show,[3,4] the octomers are formed at expense of the monomeric phase. Therefore, Eq. (2) is a better choice when comparing the relative stability between the octomers and the $\sqrt{3} \times \sqrt{3}$ arrangement. In this case, the S-FCC model served as initial state and four additional sulfur atoms became further adsorbed in order to form the rectangles. The adsorption energies calculated in this way showed that each additional sulfur atom lowered the energy by 3.3 eV (in average) when forming the rectangular patterns (see Table I), which entirely agrees with the spontaneous formation of these structures.[7–12]

The average sulfur-sulfur distances for the dimers adsorbed on Au(111) varied from 2.02 to 2.05 Å (see Table I), which were larger than the calculated distance for an isolated dimer (1.90 Å) and slightly smaller than the value for an isolated S_8 molecule (2.06 Å). Experimental values between 2.8 and 3.1 Å[3,9] are reported from direct measurements in the STM images. In consequence, these distances are an average among all neighboring sulfur atoms and not only between those that could form a dimer. Therefore, calculating average sulfur-sulfur separations among all neighboring sulfur atoms, and not only between those that formed a dimer, was a better choice for establishing comparison with the experiment. In this case, the values ranged from 2.73 to 2.85 Å (without counting O2-F which was the most deformed structure after optimization), which were fairly close to the experimental ones.

This article is copyrighted as indicated in the article. Reuse of AIP content is subject to the terms at: http://scitation.aip.org/termsconditions. Downloaded to IP: 128.131.138.244 On: Wed, 30 Jul 2014 14:47:22

The octomer size was taken as the distance among sulfur atoms placed in the corners of a single rectangle. Measured in this way, the sizes of the nine proposed octomers ranged between 5.27 and 6.03 Å, in good agreement with the experimental values[3,9,10] which range from 5.01 ± 0.1 to 6.2 ± 0.3 Å. The only exception was S1-S7 distance in the O2-F model: 3.99 Å (see Figure 4 for sulfur atoms numeration).

The sulfur-gold distance was directly affected by the sulfur-sulfur association, i.e. the average value for sulfur atoms close to top positions was 2.40 Å, which is practically equal to the sulfur-gold distance in S-FCC and 0.17 Å larger than in S-TOP. Similarly, the average sulfur-gold distance for sulfur atoms close to bridge positions was 2.45 Å, which is 0.06 Å and 0.1 Å larger than in S-FCC and S-BRD, respectively. Furthermore, the average sulfur height for the octomers over the surface was 2.20 Å, 0.1 Å larger than the average height of the sulfur atoms in the S-TOP system. Therefore, the sulfur-sulfur association induces the elongation of sulfur-gold bond, which weakens the sulfur-gold interaction. Nevertheless, this interaction should be crucial for octomers formation since the rectangles are represented here as sulfur aggregates directly adsorbed to the surface gold atoms at specific positions.

The adsorption of sulfur atoms on the Au(111) surface to form the $\sqrt{3} \times \sqrt{3}$ lattice implies that the smallest sulfur-sulfur distance is about 5 Å. So, the direct interaction among sulfur atoms can be neglected and their valence is saturated only through hybridization with the superficial gold states. When the coverage is doubled (from 0.33 in the $\sqrt{3} \times \sqrt{3}$ lattice to 0.67 ML in the tested models for the octomers), the interaction among the sulfur atoms cannot be neglected anymore and, as it was obtained by the structural optimizations, entities formed by two or more sulfur atoms separated by sulfur-sulfur bond distances are the most stable species on the surface; the formation of the octomers was satisfactorily explained using sulfur dimers instead of monomers.

The new features that arose from the sulfur-sulfur interaction at the electronic level were analyzed through the PDOS onto S(3p) and Au(5d) states. Figures 5(a)–5(d) displays the PDOS onto the Au(5d) and S(3p) orbitals for the three monomeric systems (S-TOP, S-BRD, and S-FCC, see Figure 3) and for the dimeric system O2-B (see Figures 4). The O2-B model was selected because the sulfur dimers remained nearly perpendicular to each other in its final optimized structure. In this model two dimers stayed oriented along the $1\bar{1}0$ direction and their sulfur atoms (sulfur atoms 1, 2, 5, and 6 of O2-B in Figure 4) were mainly adsorbed to one gold atom (practically equivalent to the on-top position in the monomeric case). The other two dimers were oriented along the $11\bar{2}$ direction and one sulfur atom of each dimer (sulfur atoms 3 and 7 of O2-B in Figure 4) was adsorbed to one gold atom (on-top) and the other (sulfur atoms 4 and 8 of O2-B in Figure 4) could be considered located close to two gold atoms instead of one (equivalent to the bridge position in the monomeric case). These dimers orientations were achieved exclusively in the O2-B model and allowed, as it will be seen below, an easier analysis of PDOS curves. Figures 5(e)–5(j) also show the charge densities isosurfaces (CDI) associated to states at specific energies (±0.2 eV) within the eigenstates

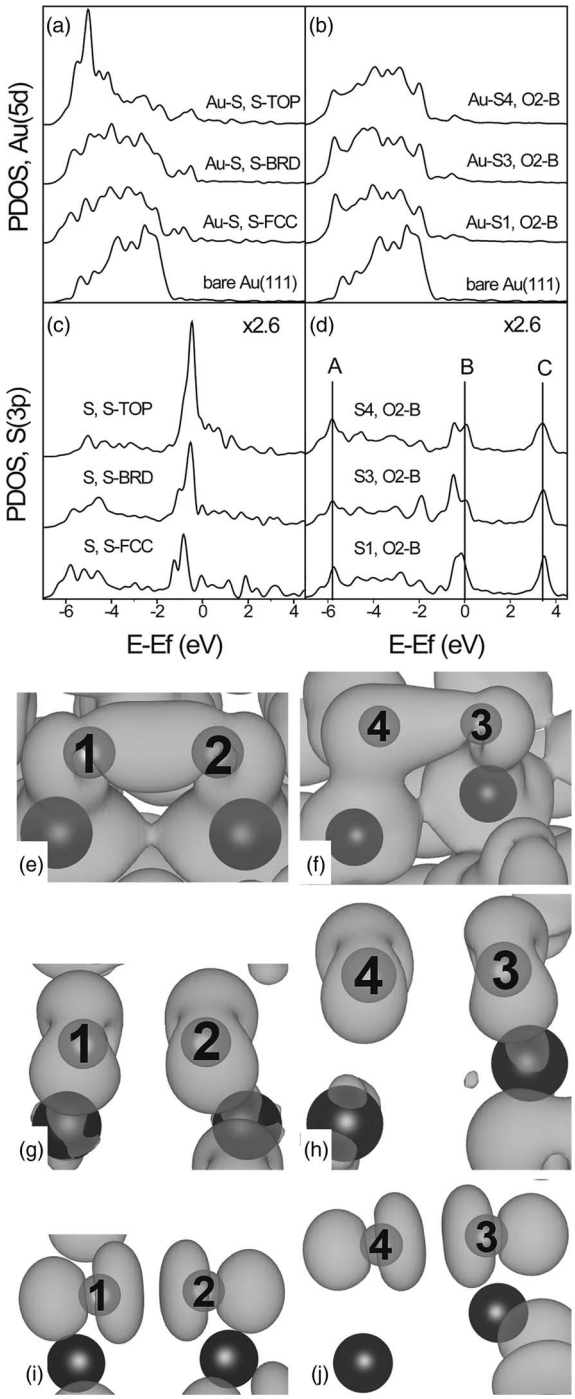

FIG. 5. Density of states projections onto the S(3p) and the Au(5d) states in S-FCC, S-BRD. S-TOP (left) and O2-B (right). (a) Au(5d) PDOS of the nearest gold atoms to the sulfur atoms in the monomeric systems, from bottom to top: bare Au(111) surface, S-FCC, S-BRD, and S-TOP. (b) Au(5d) PDOS of the nearest gold atoms to the selected sulfur atoms in the O2-B system, from bottom to top: bare Au(111) surface, nearest gold atom to sulfur 1, nearest gold atom to sulfur 3, and nearest gold atom to sulfur 4 (see Figure 4 for numeration). (c) S(3p) PDOS of the monomeric systems, from bottom to top: S-FCC, S-BRD, and S-TOP. (d) S(3p) PDOS of the O2-B system, from bottom to top: sulfur atoms 1, 3, and 4 (see Figure 4 for numeration). The vertical lines labeled as A, B, and C mark the energy range centers of those states selected to form the charge density isosurfaces (CDIs). (e)–(j) CDIs, sulfur atoms are represented by gray spheres and they are numerated according to Figure 4 from 1 to 4; the nearest gold atoms appear as black spheres. (e) and (f) CDIs of states within −5.8 ± 0.2 eV range (vertical line A). (g) and (h) CDIs of states within 0.0 ± 0.2 eV range (vertical line B). (i) and (j) CDIs of states within 3.4 ± 0.2 eV range (vertical line C). The drawings in (e)–(j) were produced with the VESTA software.[41]

This article is copyrighted as indicated in the article. Reuse of AIP content is subject to the terms at: http://scitation.aip.org/termsconditions. Downloaded to IP: 128.131.138.244 On: Wed, 30 Jul 2014 14:47:22

spectrum of the O2-B system. These selected energies are indicated in Figure 5(d) by vertical lines and labeled by capital letters from A to C.

Figure 5(a) shows the Au(5d) PDOS of the nearest gold atoms to the sulfur atoms in the S-TOP, S-BRD, and S-FCC systems (see Figure 3). The Au(5d) bands in S-BRD and S-FCC conserved a shape close to that in the bare surface but broadened and with their centers about 0.25 eV downward shifted, which indicates the deactivation of the surface gold atoms when they partially complete their truncated coordination with sulfur atoms.[34] Meanwhile, the Au(5d) band in the S-TOP system showed a dramatic transformation when it was compared with the bare surface. Its principal feature was a narrow peak located at −5.0 eV below the Fermi level, which was mainly a consequence of the projection onto the gold atomic orbitals 5dxz and 5dyz (the x and y axes were oriented along $1\bar{1}0$ and $11\bar{2}$ directions, respectively, and z was perpendicular to the surface) whose shoulder at −5.5 eV was caused by $5dz^2$ and $5dx^2$-y^2 contributions. These are indications of a strong overlapping between the sulfur and gold pairs of orbitals 3px-5dxz, 3py-5dyz, and 3pz-$5dz^2$.

In Figure 5(b) is illustrated the Au(5d) projections corresponding to the O2-B model. Here a set of three gold atoms is shown; only the S(3p) projections of sulfur atoms 1, 3, and 4 (see Figure 4 for numeration), which are depicted below, were necessary since the other five projections did not show any additional features, so the three selected gold atoms were the nearest ones to sulfur atoms 1, 3, and 4. In this case, the Au(5d) bands reported the same broadening and center shifting towards lower energies as in the monomeric systems. Even more, it can be observed around −5.7 eV that new peaks appear on the bonding edge of the Au(5d) band for those gold atoms that corresponded to sulfur atoms near to on-top positions (sulfur atoms 1 and 3 in O2-B), which in part resembled the intense peak in the S-TOP system (see Figure 5(a)) and it is an indication of relatively strong sulfur-gold interaction. Therefore, although previous works report the weakening of this interaction when the coverage and sulfur-sulfur association are increased,[7,16] dimers presence makes less active the Au(111) surface by direct interaction. However, the fundamental differences appeared when the S(3p) projections were analyzed.

The S(3p) PDOSs of the monomeric systems (S-TOP, S-BRD, and S-FCC) are shown in the Figure 5(c) and they became split in bonding and antibonding states as consequence of sulfur-gold interaction; the interaction with the metal s band broadens the adsorbate states (weak chemisorption) while the interaction with the d band provokes the mentioned splitting (strong chemisorption).[34] Within the present study the bonding states were located for the three monoatomic systems from −6.5 to 4.0 eV and the antibonding ones from −1.5 to 0.0 eV (all energies referenced to the Fermi level). Therefore, the antibonding states were occupied as consequence of the interaction with the low-energy laying Au(5d) band whose center was about 3 eV below the Fermi level.[34] As a result, the sulfur atoms adsorb on the Au(111) surface weaker than on other metals whose d band centers are shifted towards higher energies and partially occupied. This relatively weak sulfur-gold interaction favors the formation of sulfur dimers at high coverage which does not happen when the metal surface is, for example, Mo(110). The d band center of Mo(110) is above its Fermi level[34] and polyatomic sulfur species adsorbed on this surface are less stable than atomic sulfur atoms, even at high coverage.[16]

At the same time, the S(3p) PDOSs of sulfur atoms 1, 3, and 4 of the O2-B model are shown in Figure 5(d). The splitting in bonding and antibonding states was observed, although less evident than in the monomeric systems, involving now the molecular states of the dimers. The vertical line A in Figure 5(d) was located at −5.8 eV (referenced to the Fermi level), and the states within the range of energy −5.8 ± 0.2 eV were used to create the CDIs that are shown in Figures 5(e) and 5(f). As it can be clearly seen, these CDIs were closely related to bonding sulfur-sulfur σ bonds, which also enclosed the nearest gold atoms on the surface. In addition, the line B placed on 0.0 eV marked the range selected in order to form the CDIs in Figures 5(g) and 5(h); now the depicted shapes corresponded to antibonding sulfur-sulfur π bonds. In the isolated sulfur dimers the antibonding π bonds are semi-filled, which means that their α states are completely occupied while the β states are completely empty. Nevertheless, according to Figure 5(d), more than half of the projections onto α and β antibonding sulfur-sulfur π states (the peaks around 0.0 eV) were below the Fermi level, which highlights the charge transfer from the Au(111) surface to the antibonding π bonds in the dimers. This could be a reason for the elongation of the sulfur-sulfur bond distance (see Table I) when the values corresponding to the dimers on the surface (2.04 Å in average) are compared with that in the isolated molecule (1.90 Å). Finally, the vertical line C was located in the middle of the well-defined peaks at 3.4 eV above the Fermi level in Figure 5(d). The position of these peaks coincided with an energy region where the Au(5d) PDOSs of O2-B (see Figure 5(b)) did not show any relevant feature. Therefore, these states could be exclusively related with the dimeric aggregates on the surface. The CDIs that are shown in Figures 5(i) and 5(j) confirm this thought and they were formed by the contribution of the states within the energy range 3.4 ± 0.2 eV. In this case, the CDIs symmetry was unambiguously associated with antibonding sulfur-sulfur σ bonds which were far above the Fermi level, being this an additional cause for the stability of sulfur dimers on the Au(111) surface.

IV. FINAL REMARKS

The sulfur adsorption/desorption process on gold substrate is reversible from sulfide-containing alkaline solutions by using electrochemical techniques. Consequently, the transformation from the rectangular to the monomeric phase occurs when the electrochemical potential of the gold substrate decreased from −0.6 to −0.8 V (vs standard calomel electrode, SCE).[3] Under what has been reported here, this transition could be explained at least via two different ways. The first one could be thought as a partial desorption of the negative-charged dimers from the surface remaining as physisorbed species.[35] Further cleavage of the sulfur-sulfur bond could allow the readsorption of one of the sulfur atoms

This article is copyrighted as indicated in the article. Reuse of AIP content is subject to the terms at: http://scitation.aip.org/termsconditions. Downloaded to IP: 128.131.138.244 On: Wed, 30 Jul 2014 14:47:22

to form the monomeric phase, remaining the other as an anion within the aqueous medium. The second plausible mechanism could be directly related with the partial occupation of the antibonding states of the sulfur dimers due to the incremented negative charge density of the gold surface. This process would destabilize the sulfur-sulfur interaction followed by the cleavage of the sulfur-sulfur bond, remaining adsorbed on the surface a neutral atom and flowing to the solution a sulfide anion. Therefore, the weakening of the sulfur-gold interaction would be the first step towards the monomeric phase in the first proposition, while the sulfur-sulfur interaction assumes this role when the second hypothesis is analyzed. However, the details of both transitions such as their possibility of occurrence and how the sulfur-gold and sulfur-sulfur interactions are weakened together with the sulfur-sulfur bond cleavage deserve further research taking as base the models presented in this work.

Additionally, the results already reported here could provide insights for a better understanding of etch pits formation. The presented simulation highlights the necessity of a flat Au(111) surface, with the minimum of defects, for the development of rectangular patterns. This flat surface gives the ideal rearrangement of gold atoms where the stabilization of the dimers on top and bridge positions may take place. Simultaneously, when the STM experiments show pits of monoatomic[5–7] and diatomic[7] depth, its high resolution images evidence the presence of octomers inside and outside these pits.[11] Therefore the reconstruction of the gold surface after sulfur adsorption should involve only the first and possibly the second layer, leaving practically intact the deeper ones which allows the formation of rectangles inside the depression. Consequently, the generation of etch pits should be directly related with the relaxation of the herringbone reconstruction of the Au(111) surface.[36,37] The ejected gold atoms can readsorb at the step edges increasing the area of upper layers[38] or nucleate in nanometer-sized gold islands,[39] being these the outer-pits regions where the octomers are formed. The relatively weak sulfur-gold interaction could be a key feature in etch pits formation because it would induce the gold atoms to relax from the herringbone reconstruction but without hindering their way towards the step edges or their aggregation into islands. Accordingly, the study of pit formation would require bigger models[40] that take into account the relaxation of the herringbone reconstruction by the adsorption of sulfur atoms.

V. CONCLUSIONS

In the present work we have presented an extended DFT study of the rectangular patterns that are observed in real STM images. Four sulfur dimers were used to form nine different rectangular arrangements whose simulated STM images were in good agreement with the experimental ones. Furthermore, sulfur dimers made the octomers no rigid structures, allowing different rearrangements of these dimers which produced deformation in the rectangular patterns.

The PDOS analysis showed that dimers at high coverage as well as monoatomic sulfur at low coverage broadened and downward shifted the Au(5d) band at the same extent. That means, although sulfur-gold interaction decreases with coverage increments, it continues being effective and relatively strong. Besides, sulfur-sulfur bond elongation was associated with charge transfer from the Au(111) surface to the antibonding sulfur-sulfur π states which were located near the Fermi level.

The orientation of the dimers, which allowed the formation of the octomers, was highly controlled by the surface adsorptions sites. So, more experimental and theoretical studies must be oriented to verify the possibility of octomers multilayer formations because the results found here place the sulfur-gold interaction as an important point in the octomer formation. To sum up, if the octomers were an arrangement of sulfur atoms on Au(111), a fact that is very probable according to the experimental results, the rectangular patterns must be formed by combinations of dimers, trimers and also by monomers in a less extent. In this paper, we have demonstrated that the combination of dimers can produce results in good agreement with the experiments.

ACKNOWLEDGMENTS

The computational results presented have been achieved using the Vienna Scientific Cluster (VSC). The authors thank Professor Luis A. Montero-Cabrera for fruitful discussions.

[1] X. Gao, Y. Zhang, and M. J. Weaver, J. Phys. Chem. **96**, 4156 (1992).
[2] G. Andreasen, C. Vericat, M. E. Vela, and R. C. Salvarezza, J. Chem. Phys. **111**, 9457 (1999).
[3] C. Vericat, G. Andreasen, M. E. Vela, and R. C. Salvarezza, J. Phys. Chem. B **104**, 302 (2000).
[4] C. Vericat, M. E. Vela, G. Andreasen, R. C. Salvarezza, L. Vázquez, and J. A. Martín-Gago, Langmuir **17**, 4919 (2001).
[5] M. M. Biener, J. Biener, and C. M. Friend, Langmuir **21**, 1668 (2005).
[6] M. M. Biener, J. Biener, and C. M. Friend, Surf. Sci. **601**, 1659 (2007).
[7] P. G. Lustemberg, C. Vericat, G. A. Benitez, M. E. Vela, N. Tognalli, A. Fainstein, M. L. Martiarena, and R. C. Salvarezza, J. Phys. Chem. C **112**, 11394 (2008).
[8] K. M. Koczkur, E. M. Hamed, and A. Houmam, Langmuir **27**, 12270 (2011).
[9] A. Houmam, K. M. Koczkur, G. Moula, and E. M. Hamed, Chem. Phys. Chem. **13**, 1240 (2012).
[10] A. Houmam, H. Muhammad, and K. M. Koczkur, Langmuir **28**, 16881 (2012).
[11] K. M. Koczkur, E. M. Hamed, C. R. Hesp, and A. Houmam, Phys. Chem. Chem. Phys. **15**, 348 (2013).
[12] K. M. Koczkur and A. Houmam, Surf. Sci. **624**, 44 (2014).
[13] S. Y. Quek, M. M. Biener, J. Biener, J. Bhattacharjee, C. M. Friend, U. V. Waghmare, and E. Kaxiras, J. Chem. Phys. **127**, 104704 (2007).
[14] J. P. Perdew and Y. Wang, Phys. Rev. B **45**, 13244 (1992).
[15] J. Bhattacharjee and U. V. Waghmare, Phys. Rev. B **73**, 121102(R) (2006).
[16] J. A. Rodriguez, J. Dvorak, T. Jirsak, G. Liu, J. Hrbek, Y. Aray, and C. González, J. Am. Chem. Soc. **125**, 276 (2003).
[17] G. Kresse and J. Hafner, Phys. Rev. B **47**, 558 (1993).
[18] G. Kresse and J. Hafner, Phys. Rev. B **49**, 14251 (1994).
[19] G. Kresse and J. Furthmüller, Phys. Rev. B **54**, 11169 (1996).
[20] G. Kresse and J. Furthmüller, Comput. Mater. Sci. **6**, 15 (1996).
[21] J. P. Perdew, K. Burke, and M. Ernzerhof, Phys. Rev. Lett. **77**, 3865 (1996).
[22] S. Grimme, J. Comput. Chem. **27**, 1787 (2006).
[23] K. Toyoda, I. Hamada, K. Lee, S. Yanagisawa, and Y. Morikawa, J. Chem. Phys. **132**, 134703 (2010).
[24] P. E. Blöchl, Phys. Rev. B **50**, 17953 (1994).
[25] G. Kresse and D. Joubert, Phys. Rev. B **59**, 1758 (1999).
[26] H. J. Monkhorst and J. D. Pack, Phys. Rev. B **13**, 5188 (1976).
[27] M. Methfessel and T. Paxton, Phys. Rev. B **40**, 3616 (1989).
[28] See http://www.p4vasp.at/ for details information about the software and its latest versions.
[29] J. Tersoff and D. R. Hamann, Phys. Rev. B **31**, 805 (1985).

This article is copyrighted as indicated in the article. Reuse of AIP content is subject to the terms at: http://scitation.aip.org/termsconditions. Downloaded to IP: 128.131.138.244 On: Wed, 30 Jul 2014 14:47:22

[30]S. Mankefors, A. Grigoriev, and G. Wendin, Nanotechnology **14**, 849 (2003).
[31]J. Gottschalck and B. Hammer, J. Chem. Phys. **116**, 784 (2002).
[32]A. D. Daigle and J. J. BelBruno, J. Phys. Chem. C **115**, 22987 (2011).
[33]P. N. Abufager, G. Zampieri, K. Reuter, M. L. Martiarena, and H. F. Busnengo, J. Phys. Chem. C **118**, 290 (2014).
[34]B. Hammer and J. K. Nørskøv, Adv. Catal. **45**, 71 (2000).
[35]C. Vericat, M. E. Vela, G. A. Andreasen, R. C. Salvarezza, F. Borgatti, R. Felici, T.-L. Lee, F. Renner, J. Zegenhagen, and J. A. Martín-Gago, Phys. Rev. Lett. **90**, 075506 (2003).
[36]P. Maksymovych, O. Voznyy, D. B. Dougherty, D. C. Sorescu, and J. T. Yates Jr., Prog. Surf. Sci. **85**, 206 (2010).
[37]C. Vericat, M. E. Vela, G. Benitez, P. Carro, and R. C. Salvarezza, Chem. Soc. Rev. **39**, 1805 (2010).
[38]G. E. Poirier, Langmuir **13**, 2019 (1997).
[39]C. E. Bach, M. Giesen, and H. Ibach, Phys. Rev. Lett. **78**, 4225 (1997).
[40]F. Hanke and J. Björk, Phys. Rev. B **87**, 235422 (2013).
[41]K. Momma and F. Izumi, J. Appl. Crystallogr. **44**, 1272 (2011).
[42]See supplementary material at http://dx.doi.org/10.1063/1.4890997 for graphics related with the variation of the slab thickness.

This article is copyrighted as indicated in the article. Reuse of AIP content is subject to the terms at: http://scitation.aip.org/termsconditions. Downloaded to IP: 128.131.138.244 On: Wed, 30 Jul 2014 14:47:22